

## STRESS ANALYSIS OF THE MULTI-LAYERED THICK CYLINDERS

Assist. Lecturer Abdul Munium Razoki Majeed Algbory  
Institute of Medical Technology (Baghdad)  
Foundation of Technical Education

### ABSTRACT

In this study, the stress analysis of the steel-aluminum compound thick cylinders under the effects of internal pressure, thermal loading and rotational loading has been carried out using the finite element method. The structure is treated as axisymmetric body, because each of the geometry and applied loads are symmetric about the longitudinal axis.

The stresses variations (Hoop, Axial, Radial, Equivalent) through the walls thickness are determined here and the results were checked using two theories of elastic failures (Tresca and Von-Mises).

The results showed that, the Hoop stresses at the inner surface is about (600 MPa) due to effect of Internal pressure, (-500 MPa) due to thermal load, (57 MPa) due to effect of rotational speed while about (150 MPa) due to the effect of the total loading.

It can be seen that the max. hoop stress concentrated at the contact surface between the two cylinders. Also the temperature distribution through the cylinder thickness has been determined.

Key word: thick cylinder, compound, temperature distribution, thermal stress

### تحليل الاجهادات الاسطوانات السميكة المتعددة الطبقات

م.م. عبدالمنعم رزوقي مجيد الجبوري  
المعهد الطبي التقني (بغداد) / هيئة التعليم التقني

#### الخلاصة

في هذه الدراسة، تم دراسة تحليل الاجهادات للاسطوانات السميكة المركبة من مادتي الفولاذ والالمنيوم تحت تأثير الضغط الداخلي والحمل الحراري والسرعة الدورانية باستخدام طريقة العناصر المحددة. تم معالجة الموضوع على انه جسم متناظر من حيث الاحمال والشكل الهندسي حول المحور الطولي.

تم حساب التغير في توزيع الاجهادات (Equivalent, Radial and Hoop) خلال سمك الجدار ودققت النتائج باستخدام نظريتي الفشل المرن وهما (Tresca, Von-Mises).

لوحظ ان الاجهادات المماسية (Hoop Stresses) في السطح الداخلي كانت (600 MPa) نتيجة الضغط الداخلي و (-500 MPa) نتيجة التأثير الحراري و (57 MPa) نتيجة السرعة الدورانية وبينما حوالي (157 MPa) نتيجة تأثير الحمل الكلي. ولوحظ ان الاجهادات المماسية العظمى نتيجة جميع الاحمال تتمركز عند سطوح التماس بين الاسطوانات. وكذلك تم دراسة توزيع درجات الحرارة خلال سمك الاسطوانة.

## INTRODUCTION

The compound mould of the centrifugal casting technique, represent the most common of the applications of the compound thick cylinder which subject to internal pressure, rotational speed and thermal loading. Therefore, an accurate and reliable technique is essential in order to obtain the stresses.

The thermal load and rotational speed are one of the most important parameters that effects on the behavior of the stress through the thickness of the compound thick cylinder and this behavior depends on the mechanical and thermal properties which, in fact, vary with the temperature variation [1].

The effect of temperature on the deformation field is not one-way phenomena. When the mechanical and thermal aspects are coupled, and inseparable.

In general, thermal stress generation can be attributed to two main causes [2, 3].

- When the temperature distribution in the body is uniform two particular causes that produces stresses: Existence of external constraints, as occurs, if when the ends of a beam are fastened within a wall. And non homogeneity of the body such as discontinuity of surfaces.
- When the temperature distribution in the body is not uniform which gives a non-uniform deformation, and a system of stresses within the body is developed when the body undergoes a thermal transient state.

**M. Jabbari et al. 2002** presented an analytical solution for the calculation of the axisymmetric thermal and mechanical stresses in thick hollow cylinder made of FGM by using navier equation [4].

**Nejad et al. 2010** shows the stress variation along the radial direction of rotating FGM cylinder subjected to internal pressure [5].

**Jahromi et al. 2010** investigated the residual stresses induced by autofrettage process in layered and functionally graded composite vessels. This study showed that the induced residual stress at the inner surface of composite vessels much higher values compared to a metal vessel counter part depending on the properties of composite constituents [6].

**Noda 1987** studied the transient thermal stresses in a transversely isotropic, semi-infinite solid circular cylinder subjected to a convection heat loss on the end surface. The theoretical analysis considered the effect of the thermal and elastic isotropic of the material properties on thermal stresses in a transversely isotropic semi-infinite circular cylinder due to cylindrical surface heat generation [7].

## THEORY

It is very important to study the temperature distribution and stress analysis of the compound thick cylinder subjected to different loading simultaneously such as internal pressure, rotational speed and thermal loading to know the behavior of stress between the single cylinder and compound cylinder.

Thick Cylinder Subjected to Internal Pressure Only [8]

From the follow equilibrium equation for thick cylinder

$$\frac{d\sigma_r}{dr} = \frac{\sigma_\theta - \sigma_r}{r} \quad (1)$$

The Lamé's equation can be derived

$$\sigma_r = A - \frac{B}{r^2}, \quad \sigma_\theta = A + \frac{B}{r^2}$$

at  $r = r_i$                        $p = p_i$

$$\sigma_r = \frac{r_i^2 p_i}{(r_o^2 - r_i^2)} \left[ 1 - \left( \frac{r_o}{r} \right) \right] \quad (2)$$

$$\sigma_\theta = \frac{r_i^2 p_i}{(r_o^2 - r_i^2)} \left[ 1 + \left( \frac{r_o}{r} \right) \right] \quad (3)$$

$$\sigma_z = \frac{\sigma_r + \sigma_\theta}{2} \quad (4)$$

Thick Cylinder Subjected to Internal Pressure and Rotational Speed [8 & 9]

$$\sigma_r = A - \frac{B}{r^2} - (3 - \nu) \frac{\rho \cdot r^2 \cdot \omega^2}{8} \quad (5)$$

$$\sigma_\theta = A + \frac{B}{r^2} - (1 - 3\nu) \frac{\rho \cdot r^2 \cdot \omega^2}{8} \quad (6)$$

While Due to Thermal Loading [8 & 9]

Also the temperature rise of the thick cylinder will lead to induce thermal stresses.

$$\sigma_r = \frac{\alpha \cdot E}{1 - \nu} \cdot \frac{1}{r^2} \left[ \frac{r^2 - r_i^2}{r_o^2 - r_i^2} \int_{r_i}^{r_o} T \cdot r \cdot dr - \int_{r_i}^r T \cdot r \cdot dr \right] \quad (7)$$

$$\sigma_\theta = \frac{\alpha \cdot E}{1 - \nu} \cdot \frac{1}{r^2} \left[ \frac{r^2 - r_i^2}{r_o^2 - r_i^2} \int_{r_i}^{r_o} T \cdot r \cdot dr + \int_{r_i}^r T \cdot r \cdot dr - T \cdot r^2 \right] \quad (8)$$

$$\sigma_z = \nu(\sigma_r + \sigma_\theta) - \alpha \cdot E \cdot T \quad (9)$$

When the model structural components are rotationally symmetric about an axis such as the pressure vessels and solid rings, and if these structures are also subjected to axisymmetric loads, a two-dimensional analysis of a unit radian of the structure yields the complete stress and strain distribution as illustrated in **Fig.(1)** [10].

At first the shape functions were developed on a master element which is defined in  $\xi, \eta$  coordinates for normal coordinates [11].

The Lagrange shape function  $N_i$ , where  $i=1, 2, \dots, 8$  are defined such that  $N_i$  is equal to unity at node  $i$  and is zero at other nodes. In particular, consider the definition of  $N_i$ :

$$N_1 = 1 \text{ at node 1}$$

$$= 0 \text{ at node 2, 3, } \dots, 8$$

This element belongs to the serendipity family of elements. The element consists of eight nodes **Fig. (2,a)** all of which are located on the boundary. In defining  $N_i$  which refer to the master element shown in **Fig. (2,b)**.

The general equation for shape functions at all corner nodes is

$$N_i = \frac{1}{4}(1 + \xi\xi_i)(1 + \eta\eta_i)(\xi\xi_i + \eta\eta_i - 1)$$

For midside nodes with  $\xi_i = 0$

$$N_i = \frac{1}{2}(1 - \xi^2)(1 + \eta\eta_i)$$

For midside nodes with  $\eta_i = 0$

$$N_i = \frac{1}{2}(1 - \xi\xi_i)(1 + \eta^2)$$

The displacement approach to the solution of finite-element problems, a method more widely used than the stress is illustrated by an axially loaded spring;

$$[K]^e \cdot \{\delta\}^e = \{F\}^e \tag{10}$$

Where:

$[K]^e$  is the element stiffness matrix

$\{\delta\}^e$  is the element displacement vector

$\{F\}^e$  is the element applied load vector

$$\begin{aligned}
 [K]^e &= \int_e [B]^T \cdot [D] \cdot [B] \cdot dv \tag{11} \\
 dv &= r \cdot d\theta \cdot dr \cdot dz \\
 &= r \cdot d\theta \cdot dA \\
 &= 2\pi \cdot r \cdot dr \cdot dz \\
 dr \cdot dz &= \det.[J] d\xi \cdot d\eta
 \end{aligned}$$

$$[K]_{16 \times 16}^e = 2 \cdot \pi \cdot \int_{-1}^{+1} \int_{-1}^{+1} [B]_{16 \times 4}^T \cdot [D]_{4 \times 4} \cdot [B]_{4 \times 16} \cdot d\xi \cdot d\eta \tag{12}$$

$[B]_{4 \times 16}$  Strain-displacement relationship matrix is given by:

$$[B]_{4 \times 16} = \begin{bmatrix}
 \frac{\partial N_1}{\partial r} & 0 & \frac{\partial N_2}{\partial r} & 0 & \dots & \dots & \frac{\partial N_8}{\partial r} & 0 \\
 0 & \frac{\partial N_1}{\partial r} & 0 & \frac{\partial N_2}{\partial r} & \dots & \dots & 0 & \frac{\partial N_8}{\partial r} \\
 \left( \frac{\partial N_1}{\partial y} + \frac{\partial N_1}{\partial r} \right) & \cdot & \cdot & \cdot & \dots & \dots & \cdot & \left( \frac{\partial N_8}{\partial y} + \frac{\partial N_8}{\partial r} \right) \\
 \frac{N_1}{r} & 0 & \frac{N_2}{r} & 0 & \dots & \dots & \frac{N_8}{r} & 0
 \end{bmatrix}$$

[D] is the elasticity matrix which is in axisymmetric is given by:

$$[D]_{4 \times 4} = \frac{E}{(1+\nu)(1-2\nu)} \cdot \begin{bmatrix} 1 & \nu & 0 & \nu \\ \nu & 1 & 0 & \nu \\ 0 & 0 & \frac{(1-2\nu)}{2} & 0 \\ \nu & \nu & 0 & 1 \end{bmatrix}$$

$$\{\delta\}^e = \begin{Bmatrix} u_1 \\ v_1 \\ u_2 \\ v_2 \\ u_3 \\ v_3 \\ \cdot \\ \cdot \\ \cdot \\ v_8 \end{Bmatrix}$$

And the load vector is given by:

$$\{F\}^e = \{P_d\}^e + \{F\}_\Omega^e + \{F\}_{th}^e \quad (13)$$

where :

$\{P_d\}^e$  -is the load vector due to distribution pressure [12]

$\{F\}_\Omega^e$  -Centrifugal load under (inertia) force per unit volume.

$\{F\}_{th}^e$  - Thermal load vector.

The load vector due to distribution pressures is given by:

$$\{P_d\}^e = \int_{-1}^1 P \cdot [N]^T \cdot \begin{Bmatrix} \frac{\partial y}{\partial \xi} \\ \frac{\partial \xi}{\partial y} \\ -\frac{\partial \xi}{\partial \xi} \end{Bmatrix} d\xi \quad (14)$$

where

$$[N] = \begin{bmatrix} N_1 & 0 & N_2 & 0 & \cdot & \cdot & \cdot & \cdot & 0 \\ 0 & N_1 & 0 & N_2 & \cdot & \cdot & \cdot & \cdot & N_8 \end{bmatrix}$$

But the centrifugal load vector (Inertial) force per unit volume depends on assumption that the center of rotation coincides with origin of the x, y axes. Therefore the radially outward body force  $P_r$  on an element area  $dA$  is given by:

$$P_r = r.\omega^2.\rho \quad (15)$$

where:

$\omega$  -is the angular velocity in rad/s

$\rho$ -is the mass per unit volume of the material

$r$ -is the radial distance from the origin to the centroid of the element area

$P_r$ - can be resolved into components parallel to x and y axes such that

$$\begin{Bmatrix} P_x \\ P_y \end{Bmatrix} = \omega^2.\rho.\begin{Bmatrix} x \\ y \end{Bmatrix}$$

where the x and y correspond to the coordinates of the centroid of the element area

$$\begin{aligned} \{F\}_\Omega &= \int \omega^2.\rho.[N]^T \begin{Bmatrix} x \\ y \end{Bmatrix} dx.dy \\ &= \int_{-1}^{+1} \int_{-1}^{+1} \omega^2.\rho.[N]^T \begin{Bmatrix} x \\ y \end{Bmatrix} .\det[J]d\xi.d\eta \end{aligned}$$

While the thermal load vector is given by [13]

$$\begin{aligned} \{F\}_{th}^e &= \int_v [B]^T . \{\sigma^\circ\} . dv \\ \{\sigma^\circ\} &= [D] . \{\varepsilon^\circ\} \end{aligned}$$

where

$\{\sigma^\circ\}$  -Thermal stress vector

$\{\varepsilon^\circ\}$  -Thermal strain vector

$$\begin{aligned} \{\sigma^\circ\} &= [\sigma_{xx}^\circ, \sigma_{yy}^\circ, \sigma_{xy}^\circ, \sigma_{zz}^\circ]^T \\ \{\varepsilon^\circ\} &= [\varepsilon_{xx}^\circ, \varepsilon_{yy}^\circ, \varepsilon_{xy}^\circ, \varepsilon_{zz}^\circ]^T \\ \{\varepsilon^\circ\} &= [\alpha.\Delta T, \alpha.\Delta T, 0, \alpha.\Delta T]^T \end{aligned}$$

$\Delta T$ -Uniform increase in temperature.

$$\{F\}_{th}^e = 2.\pi \int_{-1}^{+1} \int_{-1}^{+1} [B]^T [D] \{\varepsilon^\circ\} r \det [J] . d\xi . d\eta \quad (16)$$

## MODELING

For the finite element method analysis of the compound thick cylinder problem, the ANSYS 11 package program is adopted. This program has very efficient capabilities to perform finite element analysis of most engineering problems. Where the material properties, dimension and loads, differ from the inside and outside cylinder.

Due to symmetry only this problem treated as axisymmetric problem.

## ELEMENT SELECTED

A single type of element is used throughout this study namely the parabolic isoperimetric element, a typical two-dimensional version of which is illustrated in Fig. (2). Parabolic isotropic elements are extremely versatile, good performers and are well tried and tested. Practical experience suggests that, for a given number of total degrees of freedom in a structure, greater accuracy is achieved by used of fewer complex elements in placed of a larger number of simple elements.

## MESH GENERATION

The compound thick cylinder as previously stated is plane-strain problem or axisymmetric problem, and the first step of finite element analysis is to discretize the structure into finite elements connected at nodes. For a structure as a compound tubes, it is necessary to discretize it into a sufficient number of elements in order to obtain a reasonable accuracy. The mesh generation of the compound thick cylinder as shown in Fig.(3). Where the thickness divided into twenty of 8-node quadrilatic (parabola) isoparametric element with total of 85 nodes.

## RESULTS AND DISCUSSIONS

The problem is solved using the finite element method as axisymmetric problem with longitudinal axis for compound thick cylinder.

The finite element solution was based on the following case study.

### Case Study

Two type of material used here in the analysis (steel, aluminum). The compound thick cylinder shown in Fig.(4) used for the modeling analysis consists of two circular cylinder with varying properties and have the following specification.

### Geometry

Steel Cylinder	Aluminum Cylinder
Inner radius = 50 mm	Inner radius = 80 mm
Outer radius = 80 mm	Outer radius = 100 mm

The two cylinder are fitted without any force (The Steel cylinder fits slightly into the Aluminum one at room temperature)

### Properties [14]

Steel Cylinder	Aluminum Cylinder
$E = 207 \text{ Gpa}$	$E = 73 \text{ Gpa}$
$\nu = 0.3$	$\nu = 0.33$
$\alpha = 11.7 \cdot 10^{-6} \text{ 1/}^\circ\text{C}$	$\alpha = 23 \cdot 10^{-6} \text{ 1/}^\circ\text{C}$
$K = 35 \text{ w/m.}^\circ\text{C}$	$K = 121 \text{ w/m.}^\circ\text{C}$
$\rho = 7850 \text{ kg/m}^3$	$\rho = 3000 \text{ kg/m}^3$

**Loading** $P_1 = 300 \text{ Mpa.}$  $T_i = 250 \text{ }^\circ\text{C}$  $T_o = 25 \text{ }^\circ\text{C}$  $\omega = 1000 \text{ rad/sec.}$ 

**Fig.(5)** shows the relationship between temperature and the cylinders thickness. It is clear from this figure that the temperature is decrease with increase the radius in nonlinear relationship and in different manner for steel and aluminum that depend on thermal conductivity.

**Fig.(6, 7)** show the relationship between stresses variation (Radial, Hoop, Longitudinal and Equivalent due to Von-Misses and Tresca) and the cylinder thickness due to the thermal load.

It is clear from **Fig.(6)** that Hoop stress and Longitudinal stress increase with increase cylinder thickness and the rate of increase differ from Steel to Aluminum material depend on thermal conductivity. It can be seen from this figure that the behavior of radial stress in Steel thickness differs in Aluminum thickness.

While from **Fig.(7)** for Equivalent stress, behavior according to Tresca is higher than Von-Misses and have nonlinear relationship with cylinder thickness.

**Figs.(8,9)** show the relationship between stresses variation and the cylinder thickness due to effect of the rotational speed.

It can be seen from **Fig.(8)** that the Hoop stress and Longitudinal stress decrease with increase the cylinder thickness in different manner for the two metals used. While the Radial stress increase and then decrease to zero value.

While from **Fig. (9)** the Equivalent stress decrease with the increase the cylinder thickness and the value of Tresca is higher than Von-Misses.

**Figs.(10,11)** show the relationship between stresses variation and the cylinder thickness due to internal pressure only. It is clear from this figure that the Hoop stress decrease with increase the cylinder thickness while the longitudinal stress approximately constant and the Radial stress decrease to zero value at outer diameter. While from **Fig. (11)** the Equivalent stress decrease with increase the cylinder thickness and the Equivalent stress due to Von-Misses lower than Tresca.

**Fig. (12)** illustrate the stress variation through the cylinder thickness due to total load. It can be seen from this figure the stresses increase with increase the cylinder thickness in nonlinear relationship for Steel and Aluminum material that depend on the material properties.

**Fig.(13)** show the relationship between equivalent stress variation and the cylinder thickness due to total load. It can be seen that the Tresca behavior is higher than Von-Misses and have nonlinear relationship.

**CONCLUSIONS**

1. Temperature decreases with the increase of the radius of thick cylinder, and the behavior of temperature in steel wall differ in that in aluminum wall.
2. Stress gradient in steel wall are higher than in aluminum wall.
3. Hoop and Longitudinal stress increase with radius of thick cylinder due to effect of thermal loading while decreases with the radius due to effect of internal pressure and rotational speed.
4. Behavior of Radial stresses through the wall thickness due to effect of thermal load is verses that due to effect of rotational speed.
5. Equivalent stresses (Von-Misses and Tresca ) due to thermal load have behavior differ than the Equivalent stresses due to rotational speed and internal pressure.



6. Hoop stress at inner surface due to effect of type of loading as follow:

Type of Loading	Hoop Stress
Thermal Load	-500 Mpa
Rotational Speed	57 Mpa
Internal Pressure	600 Mpa
Total Load	157 Mpa

7. Max. Hoop stresses concentrates at the intermediate radius of the compound thick cylinder.

#### REFERENCES

- [1] Deter, G. E., "Mechanical Metallurgy", McGraw Hill Book Company, London, (1988).
- [2] Nowinski, J. L., "Theory of Thermoelasticity with Applications", Sijthoff and Noordhoff Int. pub., (1978).
- [3] Boley, B. A. and Weiner, J. H., "Theory of Thermal Stresses", John Wiley and Sons Inc.
- [4] M. Jabbari, S. Sohrabpour, M. R. Eslami, "Mechanical and Thermal Stresses in a Functionally Graded Hollow Cylinder due to Radially Symmetric Loads", International Journal of pressure vessels and Piping, Elsevier, (2002).
- [5] Gholam Hosein Rahimi and Mohammad Zamani Nejad, "Elastic Analysis of FGM Rotating Cylindrical Pressure Vessels", Journal of the Chinese Institute of Engineers, Vol. 33, No. 4, (2010).
- [6] B. H. Jahromi, A. Ajdari, H. Nayeb-Hashemi and A. Vaziri, "Autofrettage of Layered and Functionally Graded Metal-Ceramic Composite Vessels", Journal of Composite Structures, Elsevier, (2010).
- [7] Noda, N. and Ashida, F., "Three dimensional Transient Thermal Stresses of Reactor Graphite subjected to Internal Heat Generation and Asymmetric Surface Heating", Nuc. Eng. Des., Vol.100, (1987).
- [8] Hearn, E. T., "Mechanics of Materials" Vol. (2), pregamon press Ltd, (1977).
- [9] Anthony C. Fischer-Cripps, "Introduction to Contact Mechanics", Springer, New York, Second Edition, (2007).
- [10] Klans, J. Bathe, "Finite Element Procedures", prentice-Hall International, Inc., (1996).
- [11] Tirupathi, R. C. and Ashok, D. B. "Introduction to Finite Elements in Engineering", Second Edition. Printice, hall of India, (1997).
- [12] Y. K., Cheuny and MF Yeo, "A practical Introduction to Finite Element Analysis", Piiman Publishing Limited, (1979).
- [13] E. Hinton and D.R.J., Owen, "Finite Element Programming", Academic Press, (1997).

- [14] William D. Callister, J., "Material Science and Engineering An Introduction ", John Wiley and Sons, Inc., (2007).

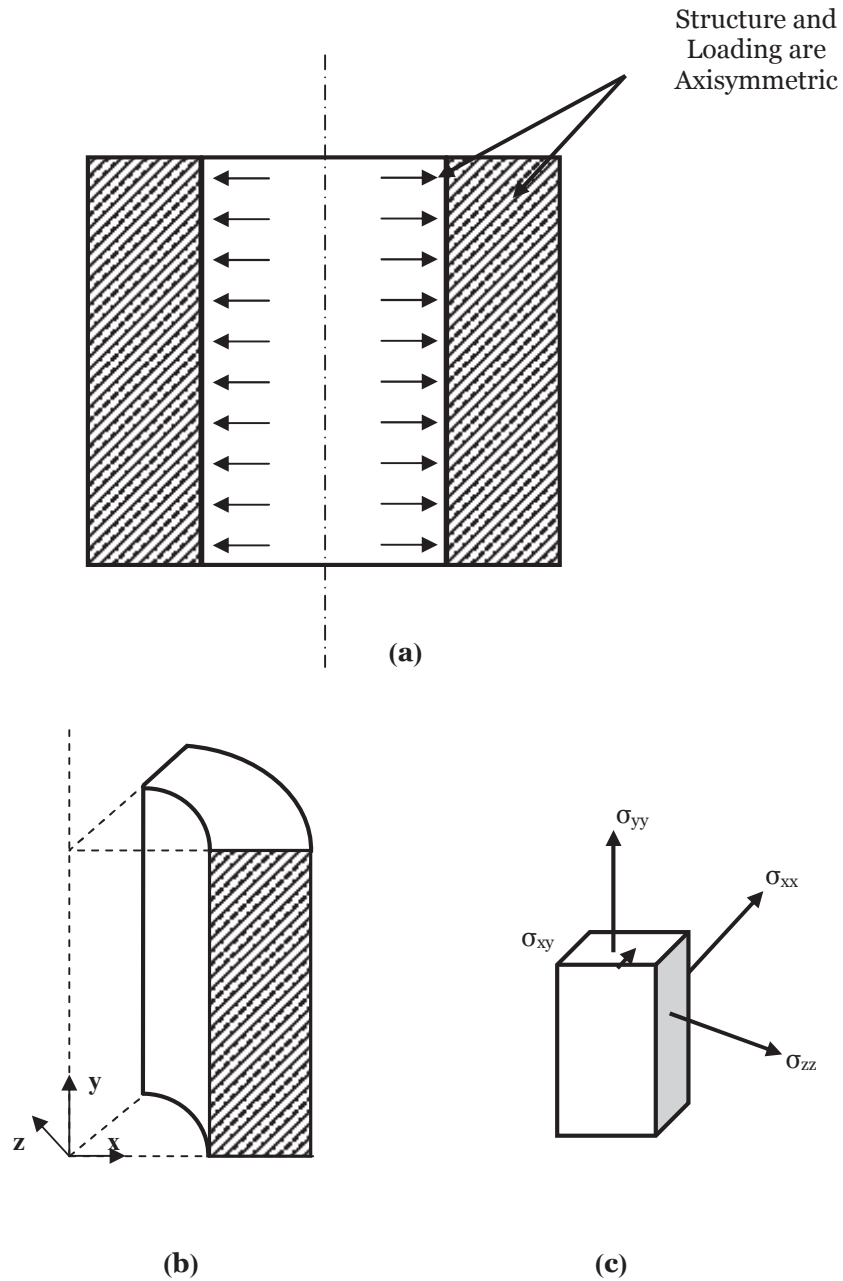


**Fig.(1)** Thick Cylinder with Symmetric Structure and Loading

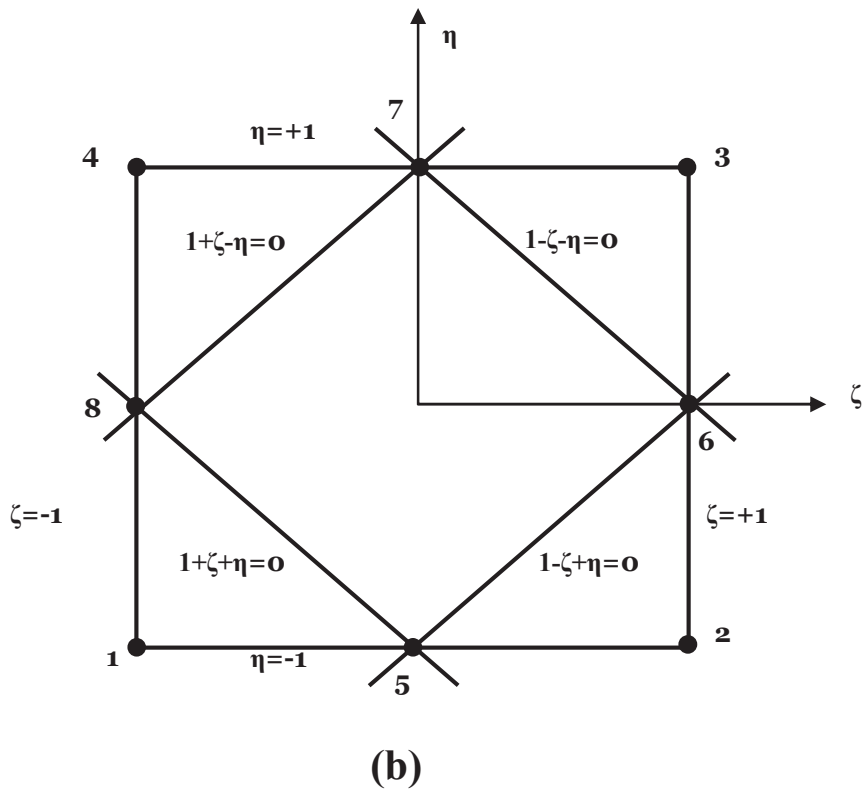
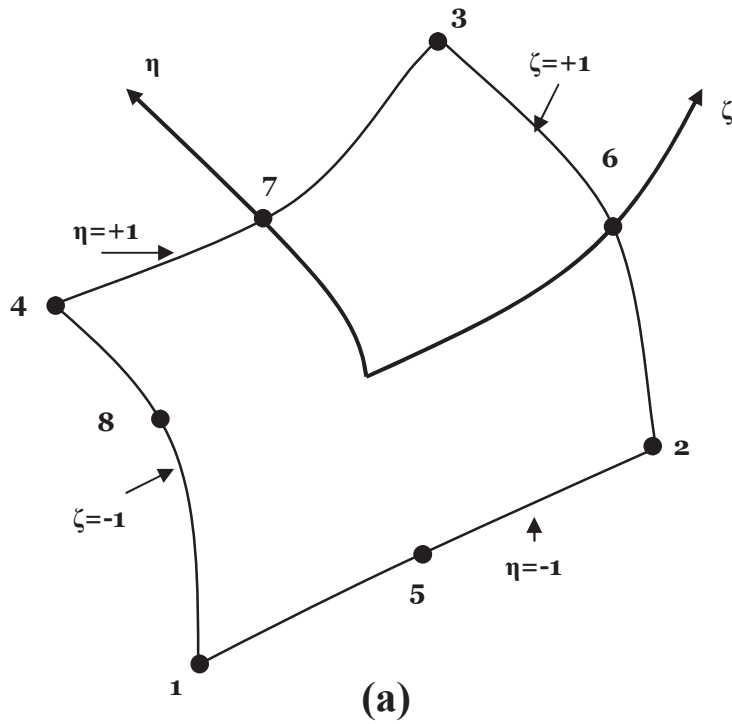


Fig.(2): 8-Node Quadrilateral Isoperimetric Element  
(a) in x,y space and (b) in  $\zeta, \eta$  space

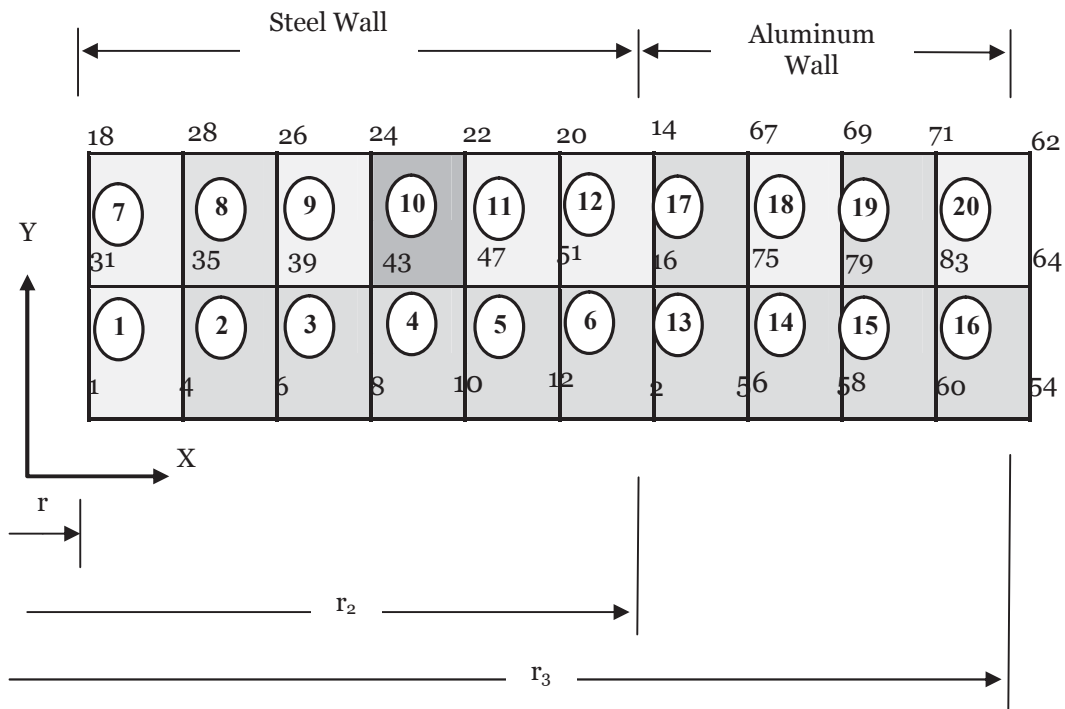


Fig. (3) Mesh Generation of Compound Thick Cylinder

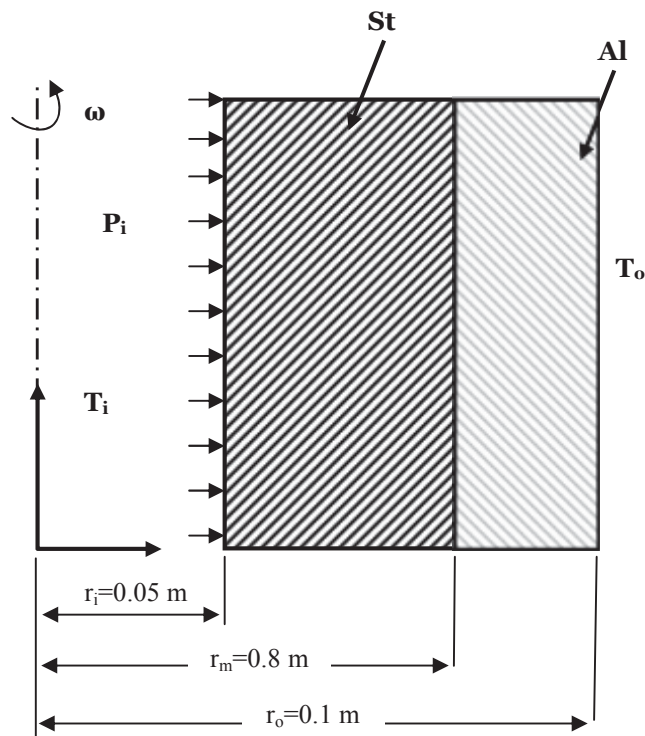
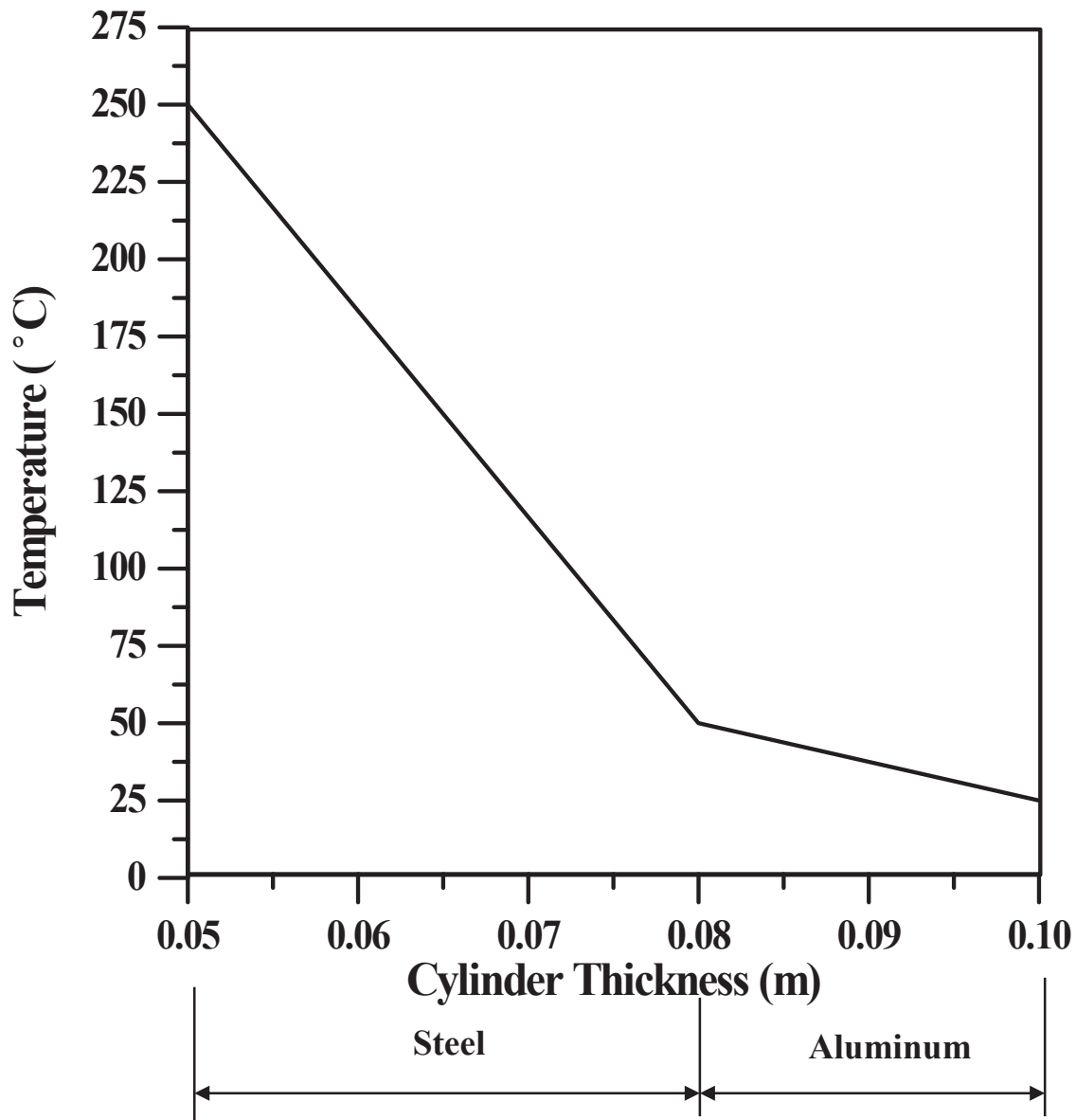


Fig. (4) Compound Thick Cylinder Cross-Section



**Fig.(5):** Temperature Distribution Through the Cylinder Thickness

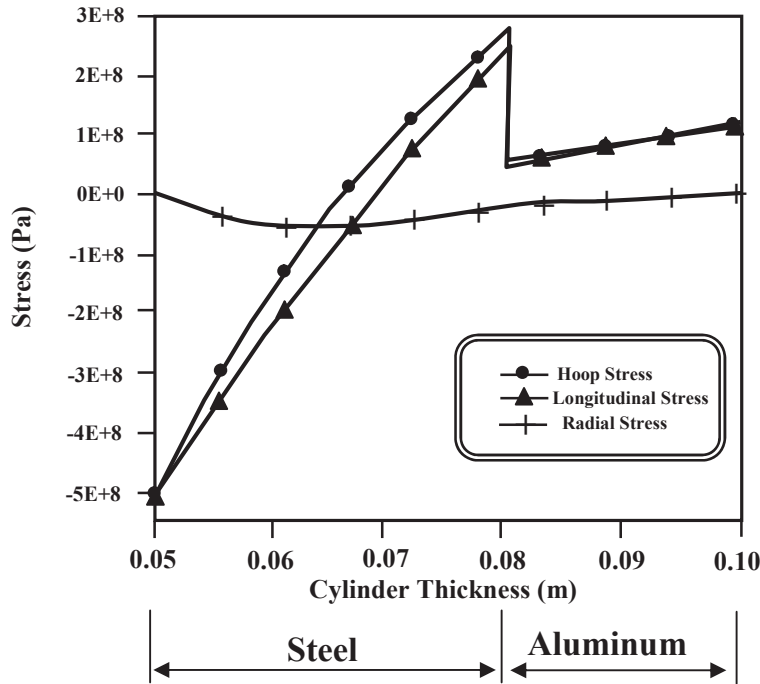


Fig.(6): Stress Variation Through the Cylinder Thickness Due to Thermal Load

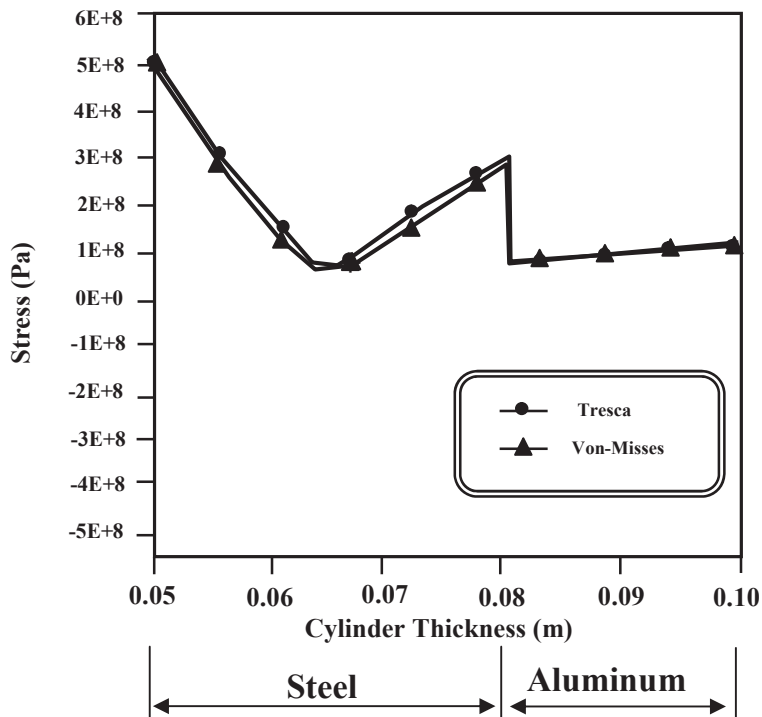


Fig.(7): Equivalent Stress Variation Through the Cylinder Thickness Due to Thermal Load

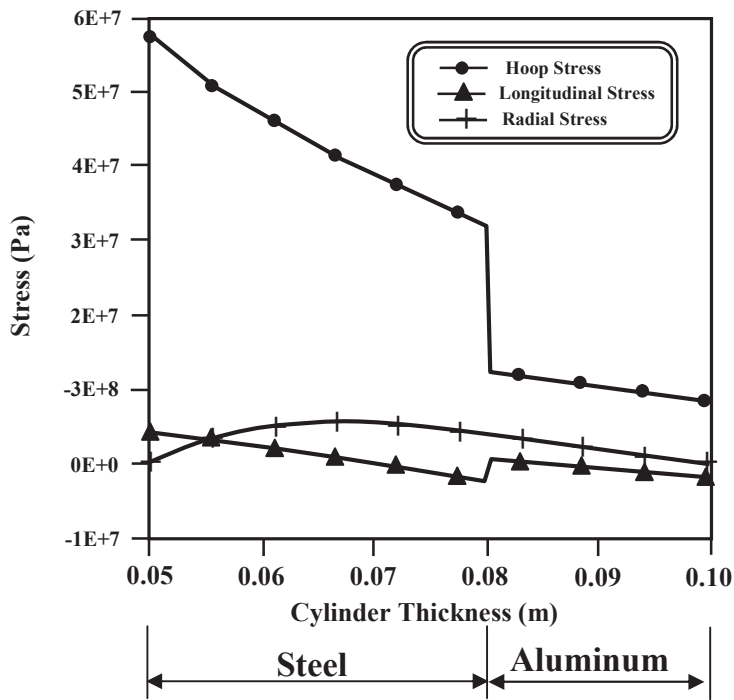


Fig.(8): Stress Variation Through the Cylinder Thickness Due to Rotational Load

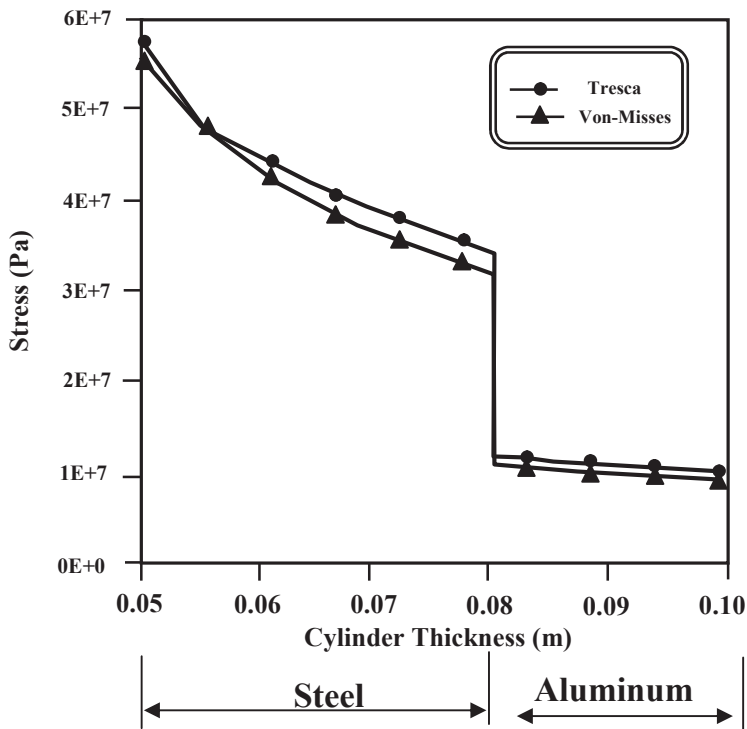


Fig.(9): Equivalent Stress Variation Through the Cylinder Thickness Due to Rotational Load

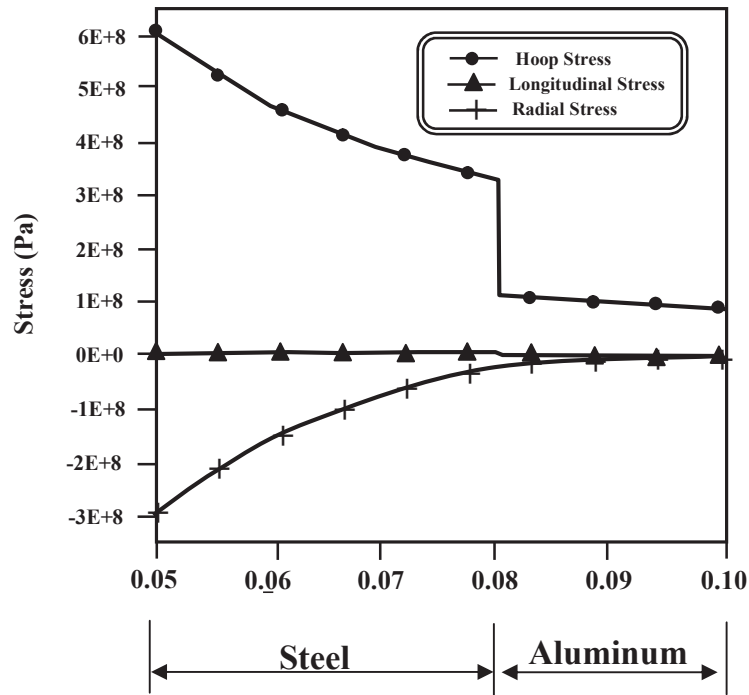


Fig.(10): Stress Variation Through the Cylinder Thickness Due to Internal Pressure

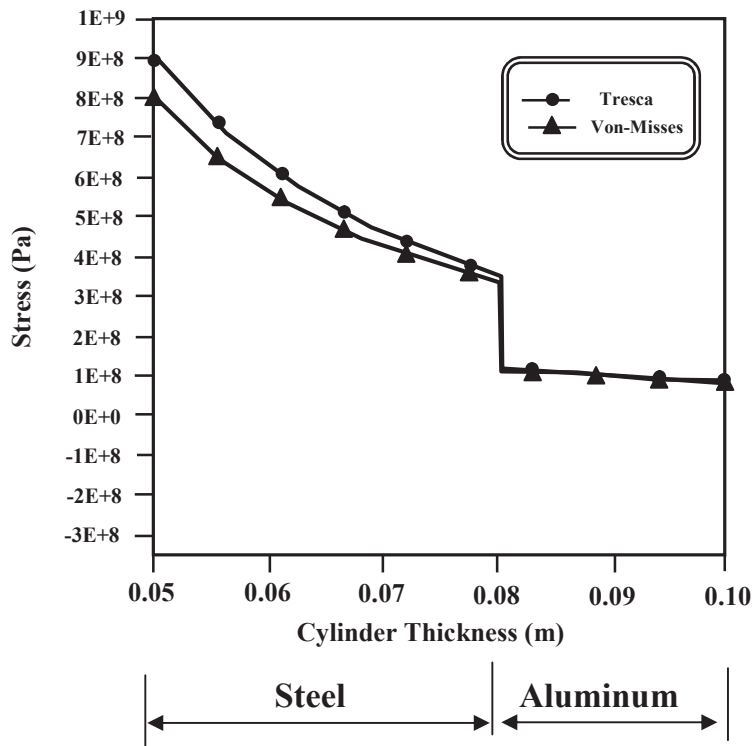


Fig.(11): Equivalent Stress Variation Through the Cylinder Thickness Due to Internal Pressure



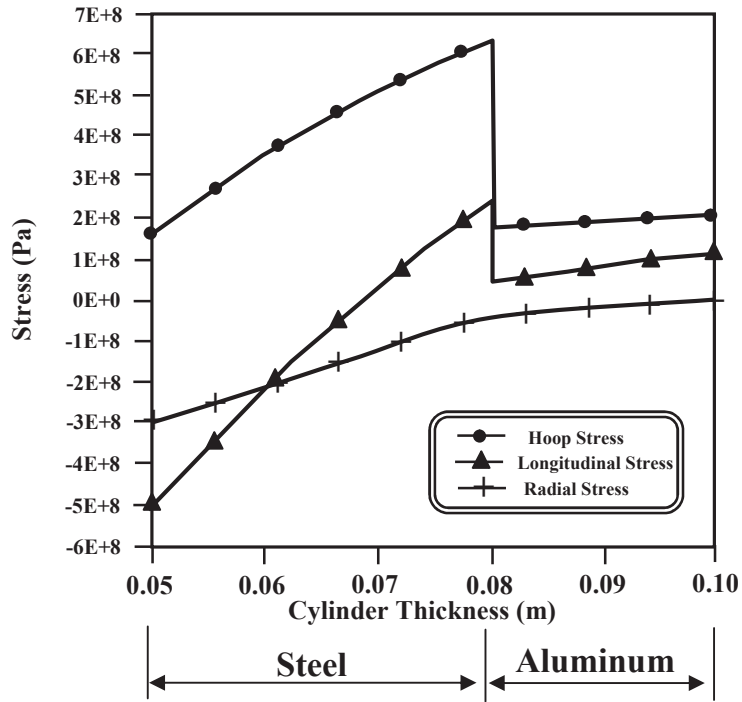


Fig.(12): Stress Variation Through the Cylinder Thickness Due to Total Load

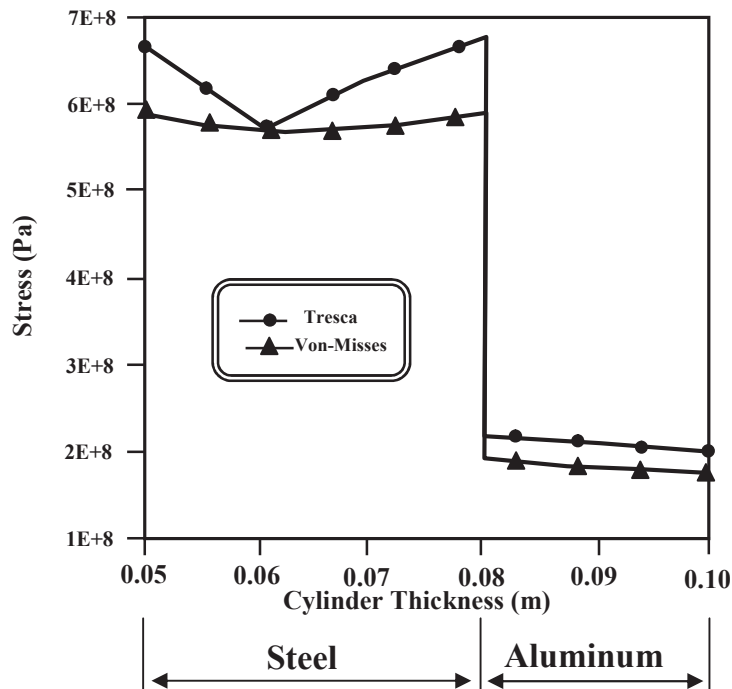


Fig.(13): Equivalent Stress Variation Through the Cylinder Thickness Due to Total Load